



HAL
open science

Vegetation reflectance spectroscopy for biomonitoring of heavy metal pollution in urban soils

Kang Yu, Maarten van Geel, Tobias Ceulemans, Willem Geerts, Miguel Marcos Ramos, Cindy Serafim, Nadine Sousa, Paula M. L. Castro, Pierre Kastendeuch, Georges Najjar, et al.

► **To cite this version:**

Kang Yu, Maarten van Geel, Tobias Ceulemans, Willem Geerts, Miguel Marcos Ramos, et al.. Vegetation reflectance spectroscopy for biomonitoring of heavy metal pollution in urban soils. *Environmental Pollution*, 2018, 243, pp.1912-1922. <10.1016/j.envpol.2018.09.053>. <hal-02625172>

HAL Id: hal-02625172

<https://hal.inrae.fr/hal-02625172v1>

Submitted on 26 May 2020

HAL is a multi-disciplinary open access archive for the deposit and dissemination of scientific research documents, whether they are published or not. The documents may come from teaching and research institutions in France or abroad, or from public or private research centers.

L'archive ouverte pluridisciplinaire **HAL**, est destinée au dépôt et à la diffusion de documents scientifiques de niveau recherche, publiés ou non, émanant des établissements d'enseignement et de recherche français ou étrangers, des laboratoires publics ou privés.



HAL Authorization

Accepted Manuscript

Vegetation reflectance spectroscopy for biomonitoring of heavy metal pollution in urban soils

Kang Yu, Maarten Van Geel, Tobias Ceulemans, Willem Geerts, Miguel Marcos Ramos, Cindy Serafim, Nadine Sousa, Paula M.L. Castro, Pierre Kastendeuch, Georges Najjar, Thierry Ameglio, Jérôme Ngao, Marc Saudreau, Olivier Honnay, Ben Somers

PII: S0269-7491(18)32356-X

DOI: [10.1016/j.envpol.2018.09.053](https://doi.org/10.1016/j.envpol.2018.09.053)

Reference: ENPO 11595

To appear in: *Environmental Pollution*

Received Date: 26 May 2018

Revised Date: 7 September 2018

Accepted Date: 9 September 2018

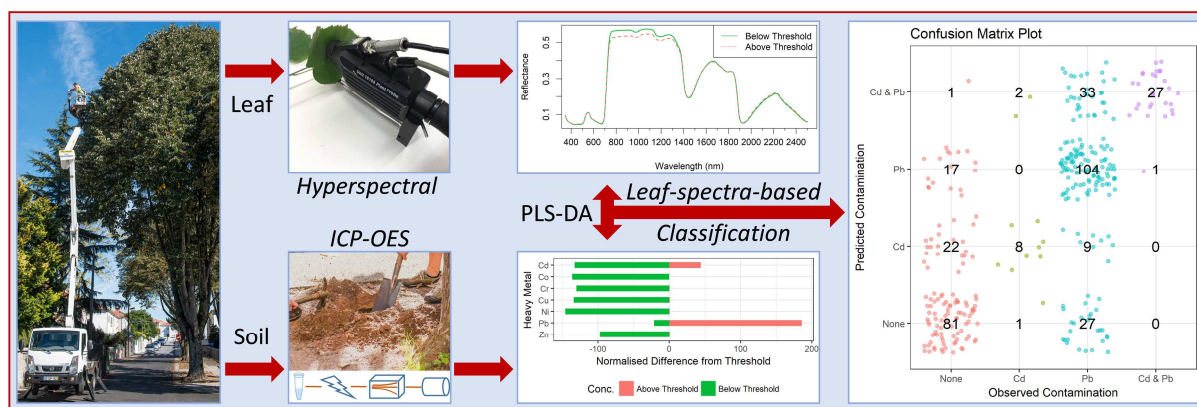


Please cite this article as: Yu, K., Van Geel, M., Ceulemans, T., Geerts, W., Ramos, M.M., Serafim, C., Sousa, N., Castro, P.M.L., Kastendeuch, P., Najjar, G., Ameglio, T., Ngao, J., Saudreau, M., Honnay, O., Somers, B., Vegetation reflectance spectroscopy for biomonitoring of heavy metal pollution in urban soils, *Environmental Pollution* (2018), doi: <https://doi.org/10.1016/j.envpol.2018.09.053>.

This is a PDF file of an unedited manuscript that has been accepted for publication. As a service to our customers we are providing this early version of the manuscript. The manuscript will undergo copyediting, typesetting, and review of the resulting proof before it is published in its final form. Please note that during the production process errors may be discovered which could affect the content, and all legal disclaimers that apply to the journal pertain.

Comment citer ce document :

Yu, K., Van Geel, M., Ceulemans, T., Geerts, W., Ramos, M. M., Serafim, C., Sousa, N., Castro, P. M. L., Kastendeuch, P., Najjar, G., Ameglio, T., Ngao, J., Saudreau, M., Honnay, O., Somers, B. (2018). Vegetation reflectance spectroscopy for biomonitoring of heavy metal pollution in urban soils. *Environmental Pollution*. 243. 1912-1922. . DOI : [10.1016/j.envpol.2018.09.053](https://doi.org/10.1016/j.envpol.2018.09.053)



Comment citer ce document :

Yu, K., Van Geel, M., Ceulemans, T., Geerts, W., Ramos, M. M., Serafim, C., Sousa, N., Castro, P. M. L., Kastendeuch, P., Najjar, G., Ameglio, T., Ngao, J., Saudreau, M., Honnay, O., Somers, B. (2018). Vegetation reflectance spectroscopy for biomonitoring of heavy metal pollution in urban soils. *Environmental Pollution*, 243, 1912-1922. . DOI : 10.1016/i.envpol.2018.09.053

Vegetation reflectance spectroscopy for biomonitoring of heavy metal pollution in urban soils

Kang Yu^{a,*}, Maarten Van Geel^b, Tobias Ceulemans^b, Willem Geerts^b, Miguel Marcos Ramos^c, Cindy Serafim^c, Nadine Sousa^c, Paula M.L. Castro^c, Pierre Kastendeuch^d, Georges Najjar^d, Thierry Ameglio^e, Jérôme Ngao^e, Marc Saudreau^e, Olivier Honnay^b and Ben Somers^a

^aDepartment of Earth & Environmental Sciences, KU Leuven, 3001, Heverlee, Belgium; E-mails: kang.yu@kuleuven.be; ben.somers@kuleuven.be

^bDepartment of Biology, KU Leuven, 3001, Heverlee, Belgium. E-mails: maarten.vangeel@kuleuven.be; tobias.ceulemans@kuleuven.be; willem.geerts@student.kuleuven.be; olivier.honnay@kuleuven.be

^cUniversidade Católica Portuguesa, CBQF - Centro de Biotecnologia e Química Fina – Laboratório Associado, Escola Superior de Biotecnologia, Rua Arquiteto Lobão Vital, 172, 4200-374 Porto, Portugal. E-mails: mmramos@porto.ucp.pt; nsousa@porto.ucp.pt; plcastro@porto.ucp.pt

^dLaboratoire des sciences de l'ingénieur, de l'informatique et de l'imagerie, Strasbourg University, Illkirch, France. E-mails: kasten@unistra.fr; georges.najjar@unistra.fr

^eUniversité Clermont Auvergne, INRA, PIAF, F-63000 Clermont Ferrand, France. E-mails: thierry.ameglio@inra.fr; jerome.ngao@inra.fr; marc.saudreau@inra.fr

*Correspondence:

Kang Yu

E-mail: kang.yu@kuleuven.be

Division of Forest, Nature and Landscape

Department of Earth and Environmental Sciences

KU Leuven

Celestijnenlaan 200e - box 2411

3001 Leuven, Belgium

Comment citer ce document :

Yu, K., Van Geel, M., Ceulemans, T., Geerts, W., Ramos, M. M., Serafim, C., Sousa, N., Castro, P. M. L., Kastendeuch, P., Najjar, G., Ameglio, T., Ngao, J., Saudreau, M., Honnay, O., Somers, B. (2018). Vegetation reflectance spectroscopy for biomonitoring of heavy metal pollution in urban soils. *Environmental Pollution*, 243, 1912-1922. . DOI : 10.1016/i.envpol.2018.09.053

1 **Abstract**

2 Heavy metals in urban soils may impose a threat to public health and may
3 negatively affect urban tree viability. Vegetation spectroscopy techniques
4 applied to bio-indicators bring new opportunities to characterize heavy metal
5 contamination, without being constrained by laborious soil sampling and lab-
6 based sample processing. Here we used *Tilia tomentosa* trees, sampled
7 across three European cities, as bio-indicators i) to investigate the impacts of
8 elevated concentrations of cadmium (Cd) and lead (Pb) on leaf mass per area
9 (LMA), total chlorophyll content (Chl), chlorophyll *a* to *b* ratio (Chl*a*:Chl*b*) and
10 the maximal PSII photochemical efficiency (Fv/Fm); and ii) to evaluate the
11 feasibility of detecting Cd and Pb contamination using leaf reflectance spectra.
12 For the latter, we used a partial-least-squares discriminant analysis (PLS-DA)
13 to train spectral-based models for the classification of Cd and/or Pb
14 contamination. We show that elevated soil Pb concentrations induced a
15 significant decrease in the LMA and Chl*a*:Chl*b*, with no decrease in Chl. We
16 did not observe pronounced reductions of Fv/Fm due to Cd and Pb
17 contamination. Elevated Cd and Pb concentrations induced contrasting
18 spectral changes in the red-edge (690~740 nm) region, which might be
19 associated with the proportional changes in leaf pigments. PLS-DA models
20 allowed for the classifications of Cd and Pb contamination, with a
21 classification accuracy of 86% (Kappa=0.48) and 83% (Kappa=0.66),
22 respectively. PLS-DA models also allowed for the detection of a collective
23 elevation of soil Cd and Pb, with an accuracy of 66% (Kappa=0.49). This

24 study demonstrates the potential of using reflectance spectroscopy for
25 biomonitoring of heavy metal contamination in urban soils.

26 **Keywords:** soil heavy metal contamination; leaf functional trait; vegetation
27 reflectance spectroscopy; red-edge position; bio-indicator

28 **Capsule**

29 Applying leaf reflectance spectroscopy to urban trees allows for biomonitoring
30 of heavy metal pollution and the classification of pollutants in urban soils.

31 **Introduction**

32 Soil contamination is a widely spread problem across Europe
33 (European Commission, 2006). Among the most frequent soil pollutants are
34 heavy metals such as arsenic (As), cadmium (Cd), chromium (Cr), copper
35 (Cu), mercury (Hg), lead (Pb), zinc (Zn), antimony (Sb), cobalt (Co) and
36 nickel (Ni), which accumulate on the soil surface and transfer to deeper soil
37 layers where they can infiltrate into the groundwater (Vince et al., 2014).
38 Plants growing on heavy metal polluted soils passively take up heavy metals,
39 jeopardizing their growth and negatively affecting other organisms feeding
40 on the plants (Panagos et al., 2013; Tóth et al., 2016). Furthermore,
41 elevated concentrations of these heavy metals in agricultural or urban soils
42 endanger food safety and public health (Poggio et al., 2009; Tóth et al.,
43 2016).

44 Urban soils typically contain elevated concentrations of Cd, Cu, Zn
45 and Pb, originating from anthropogenic activities such as traffic and industrial
46 emissions (Gallagher et al., 2008; Li et al., 2001; Poggio et al., 2009;
47 Pourkhabbaz et al., 2010; Vince et al., 2014). Cd and Pb are the most
48 common heavy metals resulting from road traffic, which is attributed to the
49 historical use of Pb as a gasoline additive (Kovarik, 2005) and Cd
50 accumulation which is mainly due to abrasion of tires (Andersson et al., 2010;
51 Vince et al., 2014). Cd and Pb are toxic for plants, animals and humans
52 (Pandit et al., 2010; Poggio et al., 2009). Cd accumulates in human body
53 and can cause nephropathy, pulmonary lesions and lung cancer after long
54 period of exposure (Poggio et al., 2009). Pb increases blood pressure and

55 damages liver, kidney and fertility, and most severely it reduces brain
56 functioning and induces hyperactivity and hearing loss in children (Poggio et
57 al., 2009). Therefore, it is vital to detect elevated concentrations of Cd and
58 Pb in urban soils.

59 Measuring heavy metals is typically based on the collection of soil or
60 road dust samples, which is labor intensive and costly, especially when
61 monitoring heavy metal contamination at larger spatial scales (Wei and Yang,
62 2010). In European countries, the estimated total annual cost related to
63 monitoring and remediating soil contaminants is 17.3 billion euros (European
64 Commission, 2006), and around 81% of the expenditures is spent on
65 remediation measures (Liedekerke et al., 2014). Consequently, only up to 15%
66 is available to be spent on site investigations (Liedekerke et al., 2014),
67 implying that there is a need for more cost-effective investigation methods to
68 evaluate spatial and temporal heterogeneity of soil pollution. Soil near-
69 infrared (NIR) spectroscopy has been applied for the detection of heavy
70 metals at relatively low cost. However, this method requires intensive soil
71 sampling (Pandit et al., 2010; Shi et al., 2014). Therefore, a spatially explicit
72 characterization of heavy metal contamination at large scales is constrained
73 by the capacity of sampling and sample processing, especially in urban areas
74 characterized by sealed soil surfaces and highly heterogeneous land-use
75 types.

76 Bio-indicators are living organisms that can be used to assess the
77 quality of the environment (Holt and Miller, 2010; Parmar et al., 2016).
78 Urban vegetation can be used as bio-indicators for monitoring air and soil

79 pollution (Ho, 1990; Khavanin Zadeh et al., 2013; Sawidis et al., 2011).
80 Plants concentrate metal elements in their above ground parts, which are
81 indicative of elevated soil heavy metal concentrations. Furthermore, heavy
82 metals can inhibit plant growth (Giulia et al., 2013; Horler et al., 1980), and
83 decrease chlorophyll content and biomass productivity (Gallagher et al., 2008;
84 Manios et al., 2003). Cd and Pb often limit plant growth by altering leaf
85 internal structures (Giulia et al., 2013; Pourkhabbaz et al., 2010). For
86 instance, Cd can reduce cell wall extensibility and relative water content
87 (Barceló and Poschenrieder, 1990). Pb can reduce not only the leaf
88 expansion but also the total chlorophyll content and efficiency of PSII electron
89 transport (Kastori et al., 1998). Overall, heavy metal toxicity causes multiple
90 direct and indirect effects on various physiological functions and on the
91 morphology of plants (Barceló and Poschenrieder, 1990), reflected in
92 changes of leaf functional traits.

93 Metal induced morphological and physiological changes can further
94 alter vegetation absorbance and reflectance characteristics (Horler et al.,
95 1980). Typically, heavy metal contamination induces most notable changes
96 in the visible and NIR spectral regions, and thus reflectance spectroscopy
97 holds great promise for evaluating the impact of heavy metal contamination
98 on vegetation (Clevers et al., 2004; Kooistra et al., 2004, 2003; Rosso et al.,
99 2005). By applying reflectance spectroscopy to monitoring candidate bio-
100 indicators located at multiple sites in urban areas, researchers have been
101 able to detect polluted sites (Khavanin Zadeh et al., 2013). Previous studies
102 have investigated the effect of individual metals on vegetation spectral

103 responses, e.g., canopy reflectance in response to manipulated pot-soil Cd
104 changes (Rosso et al., 2005). However, different metals may induce similar
105 or contrasting spectral responses (Amer et al., 2017; Horler et al., 1980;
106 Manios et al., 2003). Some studies have focused on spectral response in
107 specific spectral bands such as the red-edge region (690~740 nm), which
108 has been used to estimate plant chlorophyll variations under stress due to
109 heavy metals (Clevers et al., 2004; Rosso et al., 2005). The red-edge
110 position (REP) is defined as the position generating the maximum slope
111 (inflection point) of the reflectance spectra (or maximum first derivative
112 reflectance) in the red-edge region (Clevers et al., 2004; Horler et al., 1983),
113 and has been found to be negatively related to soil Pb concentration (Clevers
114 et al., 2004; Kooistra et al., 2004). Overall, associating soil heavy metal
115 pollution with a range of plant functional and reflectance characteristics
116 provides a cost-effective method for assessing heavy metal pollution.
117 However, there is still a lack of vegetation reflectance spectroscopy studies
118 that bio-monitor Cd and Pb contamination across a variety of urban
119 environments, especially for monitoring contamination due to multiple metals.

120 Here we tested *Tilia tomentosa* as a bio-indicator for elevated soil Cd
121 and Pb concentrations. Selecting 187 study trees cross three European cities
122 (Leuven, Porto and Strasbourg), our objectives were: i) to assess the
123 impacts of elevated concentrations of Cd and Pb on leaf mass per area (LMA),
124 total chlorophyll content (Chl), chlorophyll *a* to *b* ratio (Chl_a:Chl_b) and the
125 maximal PSII photochemical efficiency (F_v/F_m); and ii) to investigate the

126 feasibility of using leaf reflectance spectroscopy and partial-least-squares
127 discriminant analysis for biomonitoring soil Cd and Pb contamination.

128 **Materials and Methods**

129 *Sampling of leaf and soil and heavy metal measurements*

130 We conducted soil and leaf sampling in summer 2017 and randomly selected
131 19 sites and 187 *T. tomentosa* trees across three medium sized cities
132 (Leuven (Belgium): n = 64; Porto (Portugal), n = 67; Strasbourg (France): n
133 = 56). We randomly selected trees for sampling, and the trunk diameter
134 ranged 5-130 cm. For each tree, we sampled the top soils (0–10 cm) at three
135 random locations surrounding the trunk, and the three locations are mixed
136 for metal measurements. We sampled 15 leaves at three random positions in
137 each tree and stored the leaf samples in a cool box with ice. We performed
138 soil sampling once, while leaf sampling was performed multiple times
139 throughout the growing season for a subset of trees in Leuven and
140 Strasbourg.

141 Heavy metal concentrations in the soil were measured by digesting 50
142 mg of dried and sieved soil with 7.5 ml concentrated hydrochloric acid and
143 2.5 ml concentrated nitric acid. The digested solution was diluted to 10 ml
144 and measured with ICP-OES. For quality control of soil metal analysis, an
145 internal soil standard was run parallel with the soil samples, which deviated
146 less than 5% of the known composition. In this study, we focused on Cd and
147 Pb, as these were the heavy metals that reached the toxicity thresholds
148 (Table 1).

149 *Identification of contamination based on soil heavy metal thresholds*
150 Soil heavy metal contamination levels were identified based on published
151 threshold standards (Tóth et al., 2016) released by the Ministry of the
152 Environment, Finland (MEF, 2007). We grouped the samples into two classes
153 - non-contaminated and contaminated, subjected to individual metals (Table
154 1). Soil samples and corresponding leaf spectral observations (section 2.3)
155 were grouped into four classes according to Pb contamination following the
156 MEF standard (MEF, 2007). The four classes included class 0 being non-
157 contaminated ($Pb < 60$ mg/kg), class 1 of low contamination ($60 \leq Pb < 200$
158 mg/kg), class 2 of medium contamination ($200 \leq Pb < 750$ mg/kg) and class
159 3 of high contamination ($Pb \geq 750$ mg/kg).

160 We also defined four contamination classes subjected to both Cd and
161 Pb contamination by re-grouping of the Cd and Pb binary classes (Table S1),
162 i.e., four Cd x Pb classes including the non-contaminated (class 0), Cd
163 contaminated only (class 1), Pb contaminated only (class 2) as well as when
164 both Cd and Pb are over the thresholds (class 3).

165 *Leaf reflectance and functional traits*

166 Leaf reflectance was measured using an ASD FieldSpec 3 spectroradiometer
167 (ASD Inc., Longmont, CO, USA) connected to a Plant Probe and Leaf Clip
168 Assembly (ASD Inc., Longmont, CO, USA). It allows for reflectance
169 measurement in a spectral range of 350 – 2500nm with a band width of 1
170 nm. Next, we measured the leaf maximal PSII photochemical efficiency
171 (F_v/F_m , ratio of the variable fluorescence to the maximal fluorescence) using

172 a chlorophyll fluorescence meter (Handy PEA, Hansatech Instruments Ltd.,
173 Pentney, UK), combined with a leaf clip that allows for dark adaption (25
174 min). Then, we measured the leaf area using a flatbed scanner, followed by
175 oven dry for 3 days, allowing to determine leaf mass per area (LMA). In total,
176 aggregated per tree and sampling time, collected leave samples allowed for
177 further statistical analysis on a sample size of 333 for reflectance and
178 functional traits. The 333 observations of reflectance spectra and functional
179 traits were grouped into their contamination classes subjected to the soil
180 heavy metal contamination classes as defined in the Section 2.2.

181 A random subset of the leaf samples (n=53) were used to determine
182 the total chlorophyll (Chl) and carotenoid (Car) content. Leaf round discs with
183 a diameter of 28.6 mm were punched from the leaf samples using a paper
184 punch. Chla, Chlb and Car were extracted with a mortar and pestle in 80%
185 acetone and their concentrations determined by measuring the solution
186 absorbance (A) at wavelengths 470, 646.8 and 663.2 nm using a UV-VIS
187 spectrophotometer (Shimadzu 1650 PC, Kyoto, Japan) according to Eqs. (1-3)
188 (Lichtenthaler, 1987).

$$Chla = 12.25 * A_{663.2} - 2.79 * A_{646.8} \#(1)$$

$$Chlb = 21.50 * A_{646.8} - 5.10 * A_{663.2} \#(2)$$

$$Car = \frac{1000 * A_{470} - 1.82 * Chla - 85.02 * Chlb}{198} \#(3)$$

189 For quality control of chlorophyll analysis, we performed parallel
190 measurements in 12 samples, and the average standard error was lower
191 than 5%.

192 *Spectral and statistical analysis*

193 To highlight the metal-induced spectral variations, we calculated the
194 reflectance relative differences between group means for the contaminated
195 and non-contaminated classes subjected to Cd and Pb contamination. We
196 also applied first derivatives to the reflectance, focusing mainly on the red-
197 edge region, to derive the red-edge inflection point (REIP) and evaluate the
198 metal induced red-edge shifts (Clevers et al., 2004).

199 Partial least squares (PLS) regression is a multivariate method for
200 relating two data matrices, X and Y, i.e., explanatory and response matrices,
201 by extracting latent variables (components) to model the variations of both
202 matrices (Wold et al., 2001). The PLS regression can reduce high
203 dimensional data (e.g. hyperspectral) to a small number of latent variables
204 which serve as new predictors on which the response variable is regressed
205 (Rosipal and Krämer, 2006). Partial least squares discriminant analysis (PLS-
206 DA) is a variant used when the response variable is categorical. We used
207 PLS-DA for the classification of metal contamination classes. PLS-DA models
208 were applied to four types of data, (i) the original reflectance spectral, and
209 three pre-processed spectral data including (i) first derivative (ii), standard
210 normal variate SNV and (iii) continuum removal (CR) precede applying the
211 PLS-DA models. PLS-DA model calibration was first initiated on the entire
212 dataset for the full spectrum with 10 components. The initial model was

213 trained using a 10-fold cross-validation with 99 times of permutations,
 214 allowing for determination of the optimal number of components and the
 215 spectral bands yielding a variable importance in projection (VIP) ≥ 0.8 .

216 For an independent validation, the entire dataset was randomly split
 217 into the training and test subsets, with a sample size being 2/3 (n=215) and
 218 1/3 (n=118) of the total observations (n=333), respectively. The VIP ≥ 0.8
 219 spectral bands were then used to train and test models on the two subsets,
 220 respectively.

221 PLS-DA Model classification accuracy was evaluated using the overall
 222 accuracy (Eq. 4) and kappa coefficient (Eq. 5), as well as for assessing the
 223 classification for individual classes using the producer's (Eq. 7) and user's
 224 accuracies (Eq. 8),

$$Accuracy = (TP + TN)/(TP + TN + FP + FN) \#(4)$$

$$Kappa = \frac{p_a - p_e}{1 - p_e} \#(5)$$

$$p_e = \frac{(TN + FP) \times (TN + FN) + (FN + TP) \times (FP + TP)}{(TP + TN + FP + FN)^2} \#(6)$$

$$Producer Accuracy = TP/(TP + FP) \#(7)$$

$$User Accuracy = TP/(TP + FN) \#(8)$$

225 where the letters *T* and *F* denote *true* and *false*, respectively, and *P* and *N*
 226 denote *positive* and *negative*, respectively, p_a is the actual agreement
 227 (identical to accuracy), whereas p_e is the expected agreement by chance
 228 (random accuracy) that can be calculated as Eq. (6).

229 We used linear mixed models to test whether elevated soil heavy
230 metals affect the leaf functional traits. We defined the metal contamination
231 classes, i.e., binary or multi-class, as the fixed effect factor and defined city
232 and sampling site as random effect factors in the mixed models. All analyses
233 were performed in the R programming environment (R Core Team, 2016).
234 The R package 'lme4' (Bates et al., 2015) was used for running the mixed
235 models, and the package 'lsmeans' (Lenth, 2016) was used for post-hoc
236 analysis of pairwise comparisons between the contaminated classes based on
237 Tukey's test. PLS-DA was implemented using the package 'mixOmics' (Rohart
238 et al., 2017).

239 **Results and Discussion**

240 *Heavy metal effects on leaf functional traits*

241 Elevated Pb and Cd concentrations had a significant effect on LMA of *T.*
242 *tomentosa* trees (Table 2). Soil Cd contamination did not induce significant
243 changes in LMA (Fig. 1a), whereas Pb contamination significantly decreased
244 LMA (Fig. 1b). Generally, Cd and Pb stress leads to damages to chloroplasts
245 and thylakoid membranes in plants (Shen et al., 2016; Wu et al., 2014),
246 which often causes reduced leaf growth such as small leaf size and small
247 stomata (Shi and Cai, 2009), as well as thin cuticles of leaf surfaces
248 (Pourkhabbaz et al., 2010). Therefore, elevated Pb concentrations could have
249 reduced leaf thickness and thus decreased LMA. Cd also induces changes in
250 leaf structural properties, while Cd concentrations measured in this study
251 might still be below the threshold that induces significant inhibition of leaf
252 expansion.

253 Elevated soil Pb induced significant changes in leaf total Chl content,
254 Chla to Chlb ratio (Chla:Chlb) and Fv/Fm, whereas Cd and other metals did
255 not yield significant changes (Table 2). Decrease in leaf Chl content is often
256 associated with photoinhibition and reduction of the photosynthetic capacity
257 (Shen et al., 2016). Chla:Chlb decreased significantly along with the increase
258 in soil Pb concentration (Fig. 2), suggesting that Chla was more suppressed
259 compared to Chlb (Nie et al., 2016). Similarly, a significant reduction of
260 Chla:Chlb has been found in *Torreya grandis* (Shen et al., 2016) and *Typha*
261 *latifolia* plants (Manios et al., 2003) treated with a high concentration of Cd
262 and Pb, suggesting increases in chlorophyll hydrolysis due to the toxic effect
263 (Manios et al., 2003). Results may differ for different plant species, for
264 instance in a greenhouse environment, Horler et al. (1980) observed a
265 significant decrease of Chla:Chlb in pea leaves due to elevated Cd
266 concentrations, but no changes following elevated Pb (Horler et al., 1980).

267 Cd and Pb contamination induced a decrease in Fv/Fm (Fig. 3a, b),
268 whereas Fv/Fm appeared to be not sensitive to low-level Pb contamination
269 (Fig. 3d), suggesting that Cd and Pb stress may induce photosynthesis
270 inhibition. Similarly, Cd was found to affect Fv/Fm in the wetland plant
271 species *Salicornia virginica* (Rosso et al., 2005) and in the turf grass species
272 *Festuca arundinacea Schreb* (Huang et al., 2017). Generally, the observed
273 decrease in Fv/Fm in plants subjected to Cd/Pb stress is associated with the
274 photoinhibition of PSII, as a result of the overproduction of reactive oxygen
275 species (ROS) (Huang et al., 2017; Shen et al., 2016). However, a significant
276 decrease in Fv/Fm may not always be observable if Cd/Pb concentration does

277 not exceed a high threshold (Huang et al., 2017; Shen et al., 2016). Giulia et
278 al. (2013) found that a high soil Pb concentration did not decrease Fv/Fm in
279 *Q. ilex* plants, and they argued that these metals may not significantly alter
280 functionality of the photosynthetic apparatus. Similarly, Shi and Cai (2009)
281 reported that Fv/Fm was not affected in peanut plants treated with a high
282 concentration of Cd. Therefore, the effect of heavy metals on Fv/Fm might
283 depend largely on metal type, concentration and plant species.

284 Mixed models for multi-class Cd×Pb and Pb contamination showed
285 much more pronounced effects on LMA and Chla:Chlb than on Fv/Fm and leaf
286 total Chl content (Table 3), which suggests that heavy metals induced more
287 structural changes and proportional changes in leaf biochemicals than the
288 quantity changes of individual components. An increase in leaf total Chl
289 content and Fv/Fm was observed at a relative low-level Pb or Cd×Pb
290 contamination (Table 3), suggesting that heavy metals impose complicated
291 effects on photosynthesis and that Cd and Pb may increase the PSII quantum
292 yield within a certain range of low concentrations (Ouyang et al., 2012; Shen
293 et al., 2016).

294 The effect of soil heavy metals on leaves or the content of heavy metal
295 accumulation in the leaves might be related to the age of trees (Doganlar et
296 al., 2012). To test whether tree age difference affect the observed effects of
297 Cd and Pb on leaf functional traits in this study, we used trunk diameter as a
298 proxy of tree age and added it as an additional random factor in the mixed
299 models (Table S2 and Table S3). Results suggest that the observed effects of

300 Cd and Pb on *T. tomentosa* leaves was not significantly influenced by tree
301 age.

302 *Reflectance and first derivatives in response to heavy metals*

303 Elevated soil Cd concentrations yielded relatively large variations in leaf
304 reflectance centered at the 500, 680 and 720 nm bands (Fig. 4a), whereas
305 elevated Pb yielded large variations at the 550 and 700 nm bands (Fig. 4b).
306 In the red-edge region, Cd had a large effect on reflectance at the red-edge
307 center (~720 nm), whereas Pb had a large effect on reflectance ranging from
308 the red absorption to the beginning of the red-edge bands (680~700 nm).
309 Over the full spectrum, soil Pb contamination induced larger variations
310 ($\pm 10\%$, Fig. 4b) compared to Cd contamination ($\pm 5\%$) (Fig. 4a), which
311 might be attributed to the fact that Pb contamination was severer than Cd in
312 this study. Cd concentration was slightly higher than the threshold (1 mg/kg),
313 but was much lower than the 'low guideline' of contamination level (10
314 mg/kg) at which ecological or health risks present (Tóth et al., 2016).

315 The decrease in the NIR region (750~1400 nm) was associated with
316 elevated Cd and Pb concentrations. This might be attributed partly to the
317 decreased LMA because contaminated trees often have a much thinner outer
318 epidermal layer and thus thinner leaves (Pourkhabbaz et al., 2010), although
319 the effect of Cd on LMA observed in this study was marginal (Fig. 1). Metal-
320 induced decreases in leaf NIR reflectance might be associated mainly with
321 the changes in leaf internal structural properties which decrease the internal

322 light scattering and increase the transmittance of leaves (Horler et al., 1980;
323 Kumar et al., 2001).

324 The first derivative reflectance in the visible-to-NIR bands showed two
325 major peaks centered at 530 and 720 nm (Fig. S1). In the red-edge spectral
326 region, Cd contamination induced a shift of absorbance features towards the
327 shorter wavelengths (Fig. S1a). In contrast, Pb contamination induced a red-
328 edge shift to the longer wavelengths (Fig. S1b). In addition to the red-edge
329 bands, Pb contamination also yielded large variations in the first derivative
330 reflectance at the green bands, suggesting a more pronounced change of the
331 overall shape of reflectance (cf. Fig. 4). As shown in the first derivative
332 reflectance, Pb contamination also induced a shift in the green edges (both
333 sides of the green peak) compared to Cd contamination. This might explain
334 the observed decrease in the Chla:Chlb ratio (Fig. 2), since absorption at the
335 green edge bands is related to Chlb variations (Kumar et al., 2001).

336 The extracted REIP showed contrasting changes in the Cd and Pb
337 contaminated trees, with decreasing and increasing trends, respectively (Fig.
338 S2), which confirms the contrasting effects of Cd and Pb contamination on
339 the red-edge reflectance. Heavy-metal induced REIP changes, or red-edge
340 shifts, have been found to depend to some degree on plant species and
341 sampling sites (Kooistra et al., 2004). Normally, a decreased REIP can be
342 observed when plant stress induces a reduction in leaf total Chl content
343 (Horler et al., 1983). However, here we did not observe obvious Chl
344 reduction associated with Cd or Pb contamination. Therefore, the REIP

345 variations observed here were more likely associated with the proportional
346 changes in the Chla:Chlb ratio, in combination with changes in leaf structures.

347 *PLS-DA model calibration for binary and multi-class classifications*

348 In the binary classifications, the PLS-DA calibration models for Cd-
349 contamination classification yielded a total accuracy of 84.1~86.5% (kappa =
350 0.46~0.49, Table S4). PLS-DA models for Pb contamination yielded a total
351 accuracy of 72.7~77.8% (kappa = 0.46~0.57). For the multi-class
352 classification of Cd×Pb-mixed contamination, PLS-DA models yielded a total
353 accuracy of 43.2~66.1% (kappa = 0.24~0.49, Table S4). PLS-DA models for
354 the multi-class classification of Pb yielded a total accuracy of 52.0~64.0%
355 (kappa = 0.29~0.43). The best classifications for individual metals are
356 illustrated in confusion-matrix plots (Fig. 5).

357 The best model for Cd correctly classified the Cd class 0 with a
358 producer and use accuracy of 86% and 97%, respectively, and were 77%
359 and 43% for the Cd class 1 (Fig. 5a). The producer and use accuracy for the
360 Pb class 0 were 88% and 67%, respectively, and 77% and 90% for the Pb
361 class 1 (Fig. 5b). The best model for Cd×Pb yielded a relatively low user
362 accuracy in predicting the classes 1 and 3 (Fig. 5c), which however, accounts
363 for a very small proportion of the total observations. The best model for
364 multi-class Pb contamination yielded a relatively high producer accuracy for
365 the classes 0 and 3 (Fig. 5d), with 80% and 100%, respectively. In contrast,
366 the model yielded a higher user accuracy for the classes 0 and 1 than for the
367 classes 2 and 3. The low user accuracy for the Pb classes 2 and 3 was mainly

368 due to the small sample size of high Pb concentrations, which consists of only
369 17 and 4 observations for the classes 2 and 3, respectively.

370 Overall, the high producer accuracy, paired with relatively low user
371 accuracy for a relatively high metal concentration was rather encouraging,
372 since our models slightly tended to overestimate the observed contamination
373 rather than underestimate the elevated contamination. This implies a high
374 probability of detecting the elevated concentrations of soil heavy metals.

375 *PLS-DA model validation using full spectrum and VIP-bands*

376 Compared to model calibration accuracies, model validation based on the full
377 spectrum produced comparable accuracies (Table S5). In binary
378 classifications, models for Pb contamination yielded higher kappa coefficients
379 than the models for Cd contamination. In multi-class classifications, model
380 validation showed improved total accuracies and kappa coefficients (Table
381 S5), suggesting the potential of using calibrated PLS-DA models for detecting
382 elevated soil Cd and Pb concentrations.

383 Validation of models trained with the VIP (≥ 0.8) bands showed
384 slightly improved kappa values and total accuracies compared to the full use
385 of bands (Table S5). The importance of individual spectral bands in the
386 classification is indicated by the VIP scores for individual metals (Fig. 6). Cd
387 contamination yielded relatively high VIP scores at the red-edge (730 nm)
388 and SWIR bands (1300 nm, 1650 nm) compared to Pb contamination,
389 suggesting unique spectral responses to elevated soil Cd in these bands (Fig.
390 6). Pb contamination yielded higher VIP scores at the green (530 nm) and

391 the beginning of red-edge (700 nm), suggesting that Pb contamination
392 induced more pronounced responses in the visible bands. For the binary
393 classifications, VIP-based PLS-DA models yielded higher accuracies for Pb-
394 contamination classification ($\kappa = 0.66$) than for Cd ($\kappa = 0.39$, Table
395 S5). For multi-class classifications, the VIP-based PLS-DA models yielded
396 comparable accuracies by using a much less amount of bands compared to
397 the use of full spectral bands.

398 Model validation results showed that selecting a set of influential bands
399 ($VIP \geq 0.8$) allowed for maintaining classification accuracy and improving
400 model-use and computational efficiencies. Within a limited number of
401 observations, by randomly dividing independent training and testing subsets
402 of observations, our results suggest that spectrally calibrated PLS-DA models
403 have great potential of applying to future scenarios for monitoring heavy
404 metals.

405 *Comparison between reflectance pre-processing methods*

406 The kappa coefficient is a balanced measure compared to the use of the
407 producer-, user- and total accuracies, especially when the observations in
408 difference classes are highly imbalanced such as in this study. Hence, we
409 evaluated the three spectra-preprocessing methods according to the kappa
410 values. Model calibration and validation both showed that the first derivatives
411 yielded the highest kappa values compared to the use of the original and
412 SNV reflectance data (Table S4 and Table S5).

413 Using a different number of components might induce some degree of
414 variation in model accuracies, although we used the cross-validation (CV)
415 procedure. In addition to the CV-optimized number of components, model
416 calibration and validation were repeated by using a fixed number of
417 components (Table S6, Table S7 and Table S8). Results showed that the first
418 derivative reflectance yielded the highest kappa coefficients, followed by the
419 CR reflectance and the original reflectance (Fig. S3). The SNV reflectance did
420 not yield improvement compared to the original reflectance data, suggesting
421 that the SNV process may mask subtle spectral responses subjected to
422 individual metals. Overall, PLS-DA models based on the first derivative
423 reflectance produced the best classifications, which also suggests that heavy
424 metals have induced complicated effects on leaf biochemical and structural
425 properties that lead to light absorption changes/shifts over the full spectrum.

426 First derivative spectra of leaves have been proven to be effective in
427 eliminating background signals and for resolving overlapping spectral
428 features (Demetriades-Shah et al., 1990), which is useful to detect plant
429 stresses or estimate pigment changes (Rundquist et al., 1996; Smith et al.,
430 2004). Also, first derivative reflectance has better discrimination power
431 compared to the original reflectance by characterizing the rate of change of
432 reflectance with respect to wavelengths (Bao et al., 2013; Lassalle et al.,
433 2018; Smith et al., 2004). Typically, derivative analysis may facilitate the
434 detection of changes that might be masked in the original spectra by the
435 presence of plant intrinsic co-variations (Horler et al., 1983). For instance,
436 derivative spectra in the visible region may enable to detect subtle changes

437 in leaf pigment balance associated with physiological disorders or vegetation
438 types (Bandaru et al., 2016; Demetriades-Shah et al., 1990; Pu, 2011).

439 Derivative analysis can be particularly useful for remotely
440 biomonitoring heavy metal using reflectance spectra measured from above
441 the vegetation canopy (Wang et al., 2018). Canopy spectra first derivatives
442 eliminate the additive noises (baseline shifts) induced by illumination
443 instability, canopy structural or soil background influences (Demetriades-
444 Shah et al., 1990; Gnyp et al., 2014; Kochubey and Kazantsev, 2012; Pu,
445 2011), thereby improving the accuracy for quantification of canopy
446 biochemical or physiological changes (Jin and Wang, 2016; O'Connell et al.,
447 2014). Moreover, PLS modeling further facilitates the use of features of the
448 full derivative spectrum for the characterization of vegetation undergoing
449 changes or stresses.

450 Apparently, PLS-DA models for Pb-contamination classifications
451 exclusively produced higher kappa values than for Cd contamination
452 classifications, across different cases of spectra-preprocessing methods,
453 model calibration (Fig. S3a) and validation (Fig. S3b), as well as when using
454 a subset of VIP-bands (Fig. S3c). This can be attributed to the data
455 imbalance between the Cd- and Pb-contamination levels, which, however,
456 shows a great promise of the proposed approach for spectroscopic detection
457 of elevated soil heavy metals, given that a diverse set of observations are
458 used for model calibration.

459 **Conclusions**

460 This study used *T. Tomentosa* trees growing in three European cities as bio-
461 indicators of soil heavy metal contamination, and evaluated whether tree
462 spectra responses were able to reflect the elevated metal concentrations.
463 Results showed that elevated soil Cd and Pb concentrations led to decrease in
464 the leaf mass per area (LMA) and the chlorophyll *a* to *b* ratio (Chl*a*:Chl*b*),
465 while no significant reduction in leaf total chlorophyll (Chl) and the maximal
466 PSII photochemical efficiency (Fv/Fm). Soil Pb contamination was severer
467 and showed more pronounced effect on LMA, Fv/Fm, Chl and Chl*a*:Chl*b* than
468 did the Cd contamination in the studied sites.

469 Cd and Pb contamination induced specific changes in leaf reflectance
470 and the reflectance first derivatives, particularly in the red-edge spectral
471 region. Partial least squares discriminant analysis (PLS-DA) models calibrated
472 using leaf reflectance showed promise for detecting soil Cd and Pb
473 contamination in urban areas. PLS-DA models based on reflectance first
474 derivatives allowed for the best classification of Cd and Pb contamination.
475 This study shows that elevated soil heavy metals can be monitored by
476 measuring leaf spectra of trees. This holds great potential for mapping urban
477 heavy metal contamination by measuring urban vegetation using high-
478 resolution spectrometers onboard airborne or drone platforms. Future work
479 should investigate whether our findings can be extrapolated to broader scales
480 by using canopy level reflectance data and a diverse set of plant species as
481 bio-indicators. Multi-temporal investigations of the quantitative relationships
482 between the practical content of heavy metals in leaves and reflectance

483 spectroscopic measures are also needed to understand metal translocation
484 from soil to vegetation and for dynamic biomonitoring of heavy metal
485 contamination.

486 **Acknowledgements**

487 This research was funded through the 2015-2016 BiodivERsA COFUND call
488 for research proposals, with the national funders BelSPo (BE), FWO (BE), FCT
489 (PT) and through the project UID/Multi/50016/2013. We thank Remi
490 Chevalier, the greenery service of the Cities of Leuven, Porto (Câmara
491 Municipal do Porto) and Strasbourg for their assistance in fieldwork and
492 measurements. The authors thank Remi Chevalier and Yasmin Vanbrabant
493 for their assistance in chlorophyll analysis.

494 **Declarations of interest**

495 None.

496 **References**

- 497 Amer, M., Tyler, A., Fouda, T., Hunter, P., Elmetwalli, A., Wilson, C., Mario
498 VALLEJO-MARIN, 2017. Spectral Characteristics for Estimation Heavy
499 Metals Accumulation in Wheat Plants and Grain. *Sci. Pap. Ser. Manag.
500 Econ. Eng. Agric. Rural Dev.* 17, 47–55.
- 501 Andersson, M., Ottesen, R.T., Langedal, M., 2010. Geochemistry of urban
502 surface soils — Monitoring in Trondheim, Norway. *Geoderma* 156,
503 112–118. <https://doi.org/10.1016/j.geoderma.2010.02.005>
- 504 Bandaru, V., Daughtry, C.S., Codling, E.E., Hansen, D.J., White-Hansen, S.,
505 Green, C.E., 2016. Evaluating Leaf and Canopy Reflectance of Stressed
506 Rice Plants to Monitor Arsenic Contamination. *Int. J. Environ. Res.
507 Public. Health* 13. <https://doi.org/10.3390/ijerph13060606>
- 508 Bao, J., Chi, M., Benediktsson, J.A., 2013. Spectral Derivative Features for
509 Classification of Hyperspectral Remote Sensing Images: Experimental
510 Evaluation. *IEEE J. Sel. Top. Appl. Earth Obs. Remote Sens.* 6, 594–
511 601. <https://doi.org/10.1109/JSTARS.2013.2237758>

- 512 Barceló, J., Poschenrieder, C., 1990. Plant water relations as affected by
513 heavy metal stress: A review. *J. Plant Nutr.* 13, 1–37.
514 <https://doi.org/10.1080/01904169009364057>
- 515 Bates, D., Mächler, M., Bolker, B., Walker, S., 2015. Fitting Linear Mixed-
516 Effects Models Using lme4. *J. Stat. Softw.* 67, 1–48.
517 <https://doi.org/10.18637/jss.v067.i01>
- 518 Clevers, J.G.P.W., Kooistra, L., Salas, E.A.L., 2004. Study of heavy metal
519 contamination in river floodplains using the red-edge position in
520 spectroscopic data. *Int. J. Remote Sens.* 25, 3883–3895.
521 <https://doi.org/10.1080/01431160310001654473>
- 522 Demetriades-Shah, T.H., Steven, M.D., Clark, J.A., 1990. High resolution
523 derivative spectra in remote sensing. *Remote Sens. Environ.* 33, 55–
524 64. [https://doi.org/10.1016/0034-4257\(90\)90055-Q](https://doi.org/10.1016/0034-4257(90)90055-Q)
- 525 Doganlar, Z.B., Doganlar, O., Erdogan, S., Onal, Y., 2012. Heavy metal
526 pollution and physiological changes in the leaves of some shrub, palm
527 and tree species in urban areas of Adana, Turkey. *Chem. Speciat.*
528 *Bioavailab.* 24, 65–78.
529 <https://doi.org/10.3184/095422912X13338055043100>
- 530 European Commission, 2006. Commission staff working document -
531 Document accompanying the Communication from the Commission to
532 the Council, The European Parliament, the European Economic and
533 Social Committee and the Committee of the Regions - Thematic
534 Strategy for Soil Protection - Impact assessment of the thematic
535 strategy on soil protection {COM(2006)231 final} {SEC(2006)1165}.
536 Commission of the European Communities, Brussels.
- 537 Gallagher, F.J., Pechmann, I., Bogden, J.D., Grabosky, J., Weis, P., 2008.
538 Soil metal concentrations and productivity of *Betula populifolia* (gray
539 birch) as measured by field spectrometry and incremental annual
540 growth in an abandoned urban Brownfield in New Jersey. *Environ.*
541 *Pollut.* 156, 699–706. <https://doi.org/10.1016/j.envpol.2008.06.013>
- 542 Giulia, M., Lucia, S., Carmen, A., 2013. Heavy metal accumulation in leaves
543 affects physiological performance and litter quality of *Quercus ilex* L. *J.*
544 *Plant Nutr. Soil Sci.* 176, 776–784.
545 <https://doi.org/10.1002/jpln.201200053>
- 546 Gnyp, M.L., Miao, Y., Yuan, F., Ustin, S.L., Yu, K., Yao, Y., Huang, S., Bareth,
547 G., 2014. Hyperspectral canopy sensing of paddy rice aboveground
548 biomass at different growth stages. *Field Crops Res.* 155, 42–55.
549 <https://doi.org/10.1016/j.fcr.2013.09.023>
- 550 Ho, Y.B., 1990. *Ulva lactuca* as bioindicator of metal contamination in
551 intertidal waters in Hong Kong. *Hydrobiologia* 203, 73–81.
552 <https://doi.org/10.1007/BF00005615>

- 553 Holt, E.A., Miller, S.W., 2010. Bioindicators: Using Organisms to Measure
554 Environmental Impacts | Learn Science at Scitable. Nat. Educ. Knowl.
555 3, 8.
- 556 Horler, D.N.H., Barber, J., Barringer, A.R., 1980. Effects of heavy metals on
557 the absorbance and reflectance spectra of plants. *Int. J. Remote Sens.*
558 1, 121–136. <https://doi.org/10.1080/01431168008547550>
- 559 Horler, D.N.H., Dockray, M., Barber, J., 1983. The red edge of plant leaf
560 reflectance. *Int. J. Remote Sens.* 4, 273–288.
561 <https://doi.org/10.1080/01431168308948546>
- 562 Huang, M., Zhu, H., Zhang, J., Tang, D., Han, X., Chen, L., Du, D., Yao, J.,
563 Chen, K., Sun, J., 2017. Toxic effects of cadmium on tall fescue and
564 different responses of the photosynthetic activities in the photosystem
565 electron donor and acceptor sides. *Sci. Rep.* 7.
566 <https://doi.org/10.1038/s41598-017-14718-w>
- 567 Jin, J., Wang, Q., 2016. Hyperspectral indices based on first derivative
568 spectra closely trace canopy transpiration in a desert plant. *Ecol.*
569 *Inform.* 35, 1–8. <https://doi.org/10.1016/j.ecoinf.2016.06.004>
- 570 Kastori, R., Plesničar, M., Sakač, Z., Panković, D., Arsenijević-Maksimović, I.,
571 1998. Effect of excess lead on sunflower growth and photosynthesis. *J.*
572 *Plant Nutr.* 21, 75–85. <https://doi.org/10.1080/01904169809365384>
- 573 Khavanin Zadeh, A.R., Veroustraete, F., Buytaert, J.A.N., Dirckx, J., Samson,
574 R., 2013. Assessing urban habitat quality using spectral characteristics
575 of *Tilia* leaves. *Environ. Pollut.* 178, 7–14.
576 <https://doi.org/10.1016/j.envpol.2013.02.021>
- 577 Kochubey, S.M., Kazantsev, T.A., 2012. Derivative vegetation indices as a
578 new approach in remote sensing of vegetation. *Front. Earth Sci.* 6,
579 188–195. <https://doi.org/10.1007/s11707-012-0325-z>
- 580 Kooistra, L., Leuven, R.S.E.W., Wehrens, R., Nienhuis, P.H., Buydens, L.M.C.,
581 2003. A comparison of methods to relate grass reflectance to soil
582 metal contamination. *Int. J. Remote Sens.* 24, 4995–5010.
583 <https://doi.org/10.1080/0143116031000080769>
- 584 Kooistra, L., Salas, E.A.L., Clevers, J.G.P.W., Wehrens, R., Leuven, R.S.E.W.,
585 Nienhuis, P.H., Buydens, L.M.C., 2004. Exploring field vegetation
586 reflectance as an indicator of soil contamination in river floodplains.
587 *Environ. Pollut.* 127, 281–290. [https://doi.org/10.1016/S0269-7491\(03\)00266-5](https://doi.org/10.1016/S0269-7491(03)00266-5)
- 589 Kovarik, W., 2005. Ethyl-lead Gasoline: How a Classic Occupational
590 Disease Became an International Public Health Disaster. *Int. J. Occup.*
591 *Environ. Health* 11, 384–397.
592 <https://doi.org/10.1179/oeh.2005.11.4.384>
- 593 Kumar, L., Schmidt, K., Dury, S., Skidmore, A., 2001. Imaging Spectrometry
594 and Vegetation Science, in: van der Meer, F.D., De Jong, S.M. (Eds.),
595 *Imaging Spectrometry - Basic Principles and Prospective Applications*,

- 596 Remote Sensing and Digital Image Processing. Springer Netherlands,
597 Dordrecht, pp. 111–155. https://doi.org/10.1007/978-0-306-47578-8_5
598
- 599 Lassalle, G., Credo, A., Hédacq, R., Fabre, S., Dubucq, D., Elger, A., 2018.
600 Assessing Soil Contamination Due to Oil and Gas Production Using
601 Vegetation Hyperspectral Reflectance. *Environ. Sci. Technol.* 52,
602 1756–1764. <https://doi.org/10.1021/acs.est.7b04618>
- 603 Lenth, R.V., 2016. Least-Squares Means: The R Package lsmeans. *J. Stat.*
604 *Softw.* 69, 1–33. <https://doi.org/10.18637/jss.v069.i01>
- 605 Li, X., Poon, C., Liu, P.S., 2001. Heavy metal contamination of urban soils
606 and street dusts in Hong Kong. *Appl. Geochem.* 16, 1361–1368.
607 [https://doi.org/10.1016/S0883-2927\(01\)00045-2](https://doi.org/10.1016/S0883-2927(01)00045-2)
- 608 Lichtenthaler, H.K., 1987. [34] Chlorophylls and carotenoids: Pigments of
609 photosynthetic biomembranes, in: *Methods in Enzymology, Plant Cell*
610 *Membranes*. Academic Press, pp. 350–382.
611 [https://doi.org/10.1016/0076-6879\(87\)48036-1](https://doi.org/10.1016/0076-6879(87)48036-1)
- 612 Liedekerke, M. van, Prokop, G., Rabl-Berger, S., Kibblewhite, M., Louwagie,
613 G., European Commission, Joint Research Centre, Institute for
614 Environment and Sustainability, 2014. Progress in the management of
615 contaminated sites in Europe. Publications Office of the European
616 Union, Luxembourg.
- 617 Manios, T., Stentiford, E.I., Millner, P.A., 2003. The effect of heavy metals
618 accumulation on the chlorophyll concentration of *Typha latifolia* plants,
619 growing in a substrate containing sewage sludge compost and watered
620 with metaliferous water. *Ecol. Eng.* 20, 65–74.
621 [https://doi.org/10.1016/S0925-8574\(03\)00004-1](https://doi.org/10.1016/S0925-8574(03)00004-1)
- 622 MEF, 2007. Government Decree on the Assessment of Soil Contamination
623 and Remediation Needs (No. 214/2007). Ministry of the Environment,
624 Finland.
- 625 Nie, J., Liu, Y., Zeng, G., Zheng, B., Tan, X., Liu, H., Xie, J., Gan, C., Liu, W.,
626 2016. Cadmium accumulation and tolerance of *Macleaya cordata*: a
627 newly potential plant for sustainable phytoremediation in Cd-
628 contaminated soil. *Environ. Sci. Pollut. Res.* 23, 10189–10199.
629 <https://doi.org/10.1007/s11356-016-6263-7>
- 630 O’Connell, J.L., Byrd, K.B., Kelly, M., 2014. Remotely-Sensed Indicators of N-
631 Related Biomass Allocation in *Schoenoplectus acutus*. *PLoS ONE* 9.
632 <https://doi.org/10.1371/journal.pone.0090870>
- 633 Ouyang, H., Kong, X., He, W., Qin, N., He, Q., Wang, Y., Wang, R., Xu, F.,
634 2012. Effects of five heavy metals at sub-lethal concentrations on the
635 growth and photosynthesis of *Chlorella vulgaris*. *Chin. Sci. Bull.* 57,
636 3363–3370. <https://doi.org/10.1007/s11434-012-5366-x>
- 637 Panagos, P., Van Liedekerke, M., Yigini, Y., Montanarella, L., 2013.
638 Contaminated Sites in Europe: Review of the Current Situation Based

- 639 on Data Collected through a European Network. *J. Environ. Public*
640 *Health* 2013, 11. <https://doi.org/10.1155/2013/158764>
- 641 Pandit, C.M., Filippelli, G.M., Li, L., 2010. Estimation of heavy-metal
642 contamination in soil using reflectance spectroscopy and partial least-
643 squares regression. *Int. J. Remote Sens.* 31, 4111–4123.
644 <https://doi.org/10.1080/01431160903229200>
- 645 Parmar, T.K., Rawtani, D., Agrawal, Y.K., 2016. Bioindicators: the natural
646 indicator of environmental pollution. *Front. Life Sci.* 9, 110–118.
647 <https://doi.org/10.1080/21553769.2016.1162753>
- 648 Poggio, L., Vrščaj, B., Schulin, R., Hepperle, E., Ajmone Marsan, F., 2009.
649 Metals pollution and human bioaccessibility of topsoils in Grugliasco
650 (Italy). *Environ. Pollut.* 157, 680–689.
651 <https://doi.org/10.1016/j.envpol.2008.08.009>
- 652 Pourkhabbaz, A., Rastin, N., Olbrich, A., Langenfeld-Heyser, R., Polle, A.,
653 2010. Influence of Environmental Pollution on Leaf Properties of Urban
654 Plane Trees, *Platanus orientalis* L. *Bull. Environ. Contam. Toxicol.* 85,
655 251–255. <https://doi.org/10.1007/s00128-010-0047-4>
- 656 Pu, R., 2011. Detecting and Mapping Invasive Plant Species by Using
657 Hyperspectral Data, in: Thenkabail, P.S., Lyon, J.G., Huete, A. (Eds.),
658 Hyperspectral Remote Sensing of Vegetation. CRC Press, Boca Raton,
659 FL, p. 447.
- 660 R Core Team, 2016. R: A language and environment for statistical computing.
661 R Foundation for Statistical Computing, Vienna, Austria.
- 662 Rohart, F., Gautier, B., Singh, A., Cao, K.-A.L., 2017. mixOmics: an R
663 package for 'omics feature selection and multiple data integration.
664 *bioRxiv* 108597. <https://doi.org/10.1101/108597>
- 665 Rosipal, R., Krämer, N., 2006. Overview and Recent Advances in Partial Least
666 Squares, in: Subspace, Latent Structure and Feature Selection,
667 Lecture Notes in Computer Science. Springer, Berlin, Heidelberg, pp.
668 34–51. https://doi.org/10.1007/11752790_2
- 669 Rosso, P.H., Pushnik, J.C., Lay, M., Ustin, S.L., 2005. Reflectance properties
670 and physiological responses of *Salicornia virginica* to heavy metal and
671 petroleum contamination. *Environ. Pollut.* 137, 241–252.
672 <https://doi.org/10.1016/j.envpol.2005.02.025>
- 673 Rundquist, D.C., Han, L., Schalles, J.F., Peake, J.S., 1996. Remote
674 Measurement of Algal Chlorophyll in Surface Waters: The Case for the
675 First Derivative of Reflectance Near 690 nm. *Photogramm. Eng.*
676 *Remote Sens.* 62, 195–200.
- 677 Sawidis, T., Breuste, J., Mitrovic, M., Pavlovic, P., Tsigaridas, K., 2011. Trees
678 as bioindicator of heavy metal pollution in three European cities.
679 *Environ. Pollut.* 159, 3560–3570.
680 <https://doi.org/10.1016/j.envpol.2011.08.008>

- 681 Shen, J., Song, L., Müller, K., Hu, Y., Song, Y., Yu, W., Wang, H., Wu, J.,
682 2016. Magnesium Alleviates Adverse Effects of Lead on Growth,
683 Photosynthesis, and Ultrastructural Alterations of *Torreya grandis*
684 Seedlings. *Front. Plant Sci.* 7.
685 <https://doi.org/10.3389/fpls.2016.01819>
- 686 Shi, G., Cai, Q., 2009. Leaf plasticity in peanut (*Arachis hypogaea* L.) in
687 response to heavy metal stress. *Environ. Exp. Bot.* 67, 112–117.
688 <https://doi.org/10.1016/j.envexpbot.2009.02.009>
- 689 Shi, T., Chen, Y., Liu, Y., Wu, G., 2014. Visible and near-infrared reflectance
690 spectroscopy—An alternative for monitoring soil contamination by
691 heavy metals. *J. Hazard. Mater.* 265, 166–176.
692 <https://doi.org/10.1016/j.jhazmat.2013.11.059>
- 693 Smith, K.L., Steven, M.D., Colls, J.J., 2004. Use of hyperspectral derivative
694 ratios in the red-edge region to identify plant stress responses to gas
695 leaks. *Remote Sens. Environ.* 92, 207–217.
696 <https://doi.org/10.1016/j.rse.2004.06.002>
- 697 Tóth, G., Hermann, T., Da Silva, M.R., Montanarella, L., 2016. Heavy metals
698 in agricultural soils of the European Union with implications for food
699 safety. *Environ. Int.* 88, 299–309.
700 <https://doi.org/10.1016/j.envint.2015.12.017>
- 701 Vince, T., Szabó, G., Csoma, Z., Sándor, G., Szabó, S., 2014. The spatial
702 distribution pattern of heavy metal concentrations in urban soils — a
703 study of anthropogenic effects in Berehove, Ukraine. *Cent. Eur. J.*
704 *Geosci.* 6, 330–343. <https://doi.org/10.2478/s13533-012-0179-7>
- 705 Wang, F., Gao, J., Zha, Y., 2018. Hyperspectral sensing of heavy metals in
706 soil and vegetation: Feasibility and challenges. *ISPRS J. Photogramm.*
707 *Remote Sens.* 136, 73–84.
708 <https://doi.org/10.1016/j.isprsjprs.2017.12.003>
- 709 Wei, B., Yang, L., 2010. A review of heavy metal contaminations in urban
710 soils, urban road dusts and agricultural soils from China. *Microchem. J.*
711 94, 99–107. <https://doi.org/10.1016/j.microc.2009.09.014>
- 712 Wold, S., Sjöström, M., Eriksson, L., 2001. PLS-regression: a basic tool of
713 chemometrics. *Chemom. Intell. Lab. Syst., PLS Methods* 58, 109–130.
714 [https://doi.org/10.1016/S0169-7439\(01\)00155-1](https://doi.org/10.1016/S0169-7439(01)00155-1)
- 715 Wu, M., Wang, P.-Y., Sun, L.-G., Zhang, J.-J., Yu, J., Wang, Y.-W., Chen, G.-
716 X., 2014. Alleviation of cadmium toxicity by cerium in rice seedlings is
717 related to improved photosynthesis, elevated antioxidant enzymes and
718 decreased oxidative stress. *Plant Growth Regul.* 74, 251–260.
719 <https://doi.org/10.1007/s10725-014-9916-x>

Figure Captions

Fig. 1. Boxplots with the leaf mass per area (LMA) differences between the binary classes (0 = non-contaminated, 1 = contaminated) of (a) Cd and (b) Pb contamination, as well as among multiple classes of (c) Cd×Pb and (d) Pb contamination. Significance levels are indicated according to the post-hoc Tukey's test of the applied mixed models.

Fig. 2. Boxplots with the leaf chlorophyll a to b ratio (Chla:Chlb) differences between the binary classes (0 = non-contaminated, 1 = contaminated) of (a) Cd and (b) Pb contamination, as well as among multiple classes for (c) Cd×Pb and (d) Pb contamination. Significance levels are indicated according to the post-hoc Tukey's test of the applied mixed models.

Fig. 3. Boxplots show the chlorophyll fluorescence Fv/Fm differences between the binary classes (0 = non-contaminated, 1 = contaminated) of (a) Cd and (b) Pb contamination, as well as among multi-class classifications of (c) Cd×Pb and (d) Pb contamination. Significance levels are indicated according to the post-hoc Tukey's test of the applied mixed models.

Fig. 4. Leaf mean reflectance of the contaminated (1) and non-contaminated (0) trees subjected to (a) Cd and (b) Pb, and their reflectance relative difference $((X1-X0)/X0)$ between the contaminated and non-contaminated leaves.

Fig. 5. Predicted versus observed classes for (a) Cd binary classification, (b) Pb binary classification, (c) Cd×Pb classification and (d) Pb multi-class classification. Here the first derivative reflectance data were used for (a), (b) and (c), the original reflectance were used for (d). Numbers indicate the confusion matrix of classification.

Fig. 6. The variable importance in projection (VIP) scores for the spectral-based PLS-DA models for binary classification for Cd and Pb contamination, and for multi-class classification of Pb and Cd×Pb contamination. $VIP \geq 0.8$ highlights the spectral bands contributing significantly to the PLS-DA models.

Tables

Table 1. Measured soil heavy metal content and the threshold values for classification of contamination. Cd and Pb were the major contaminants in this study, and Pb was the only metal that reached the highline and thus Pb contamination was classified into three sub-classes.

Metal	Range (mg/kg)	Threshold (mg/kg)	Number of observations (n)			
			Class 0	Class 1/Pb 1	Pb 2	Pb 3
Cd	0-3.9	1	294	39		
Pb*	0-2170.8	60	132	201/180	17	4
Co	0-15.9	20	333	0		
Cr	0-120.9	100	327	6		
Cu	0-159.1	100	330	3		
Ni	0-76.8	50	331	2		
Zn	10-265.8	200	329	4		

*, Pb contamination sub-levels:

- 1) Low contamination ($60 \leq \text{Pb} < 200$ mg/kg);
- 2) Medium contamination ($200 \leq \text{Pb} < 750$ mg/kg);
- 3) High contamination ($\text{Pb} \geq 750$ mg/kg).

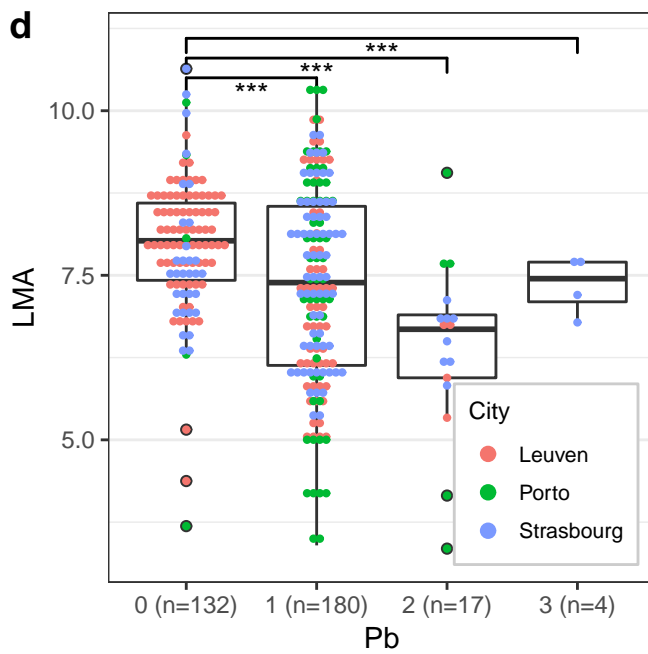
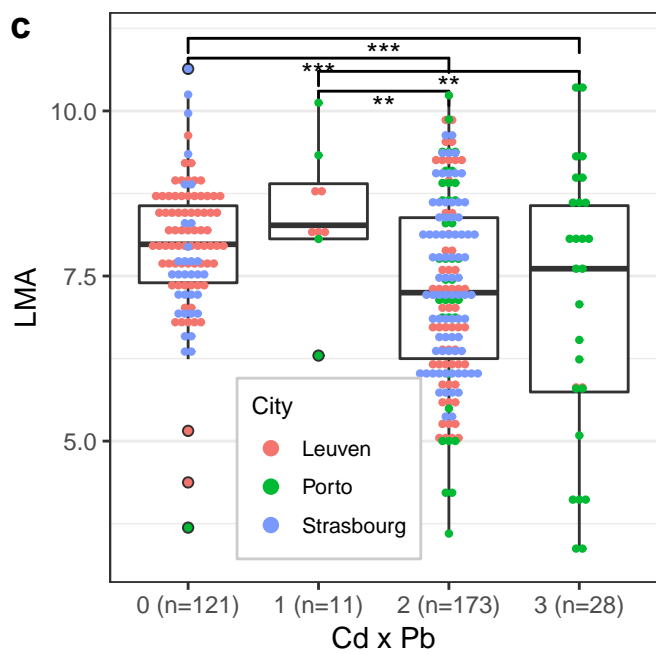
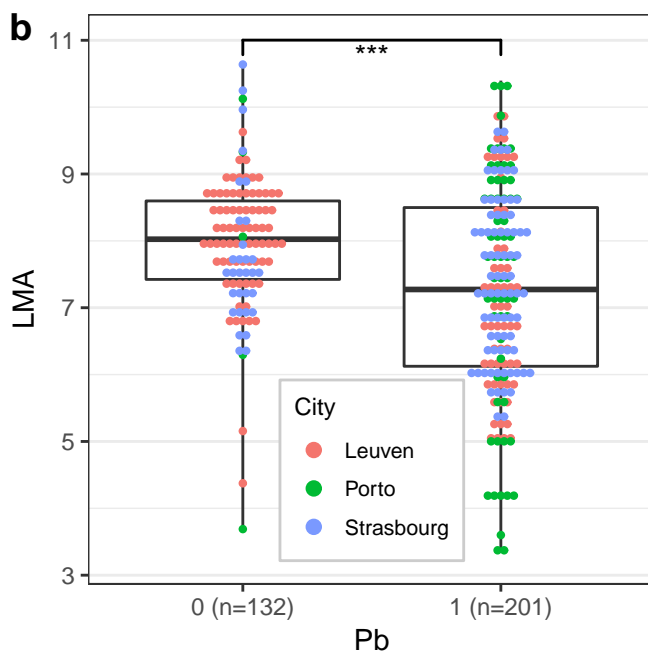
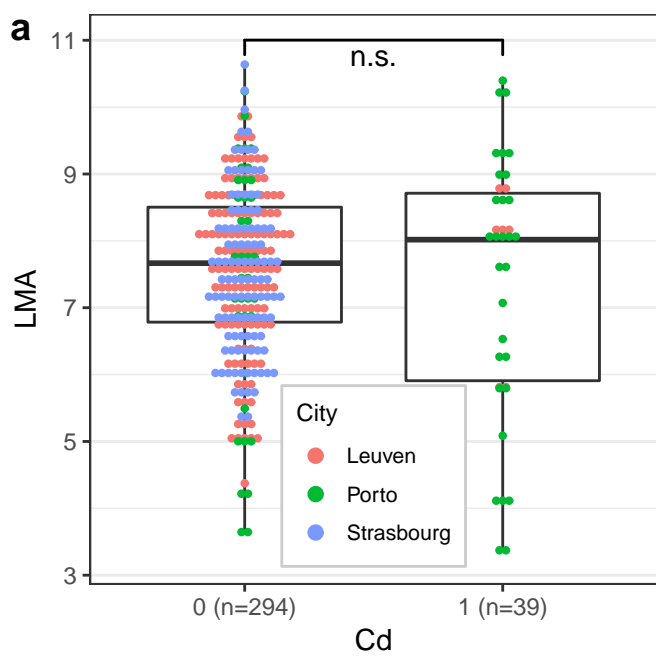
Table 2. Results of mixed models for testing the effect of soil heavy metals on leaf functional traits, including the leaf mass per area (LMA), Fv/Fm, total chlorophyll content (Chl) and Chla:Chlb ratio. Modeled random effects were city and sites. Chlorophyll data were only available for a subset of the samples, where only Cd and Pb reached the thresholds of contamination.

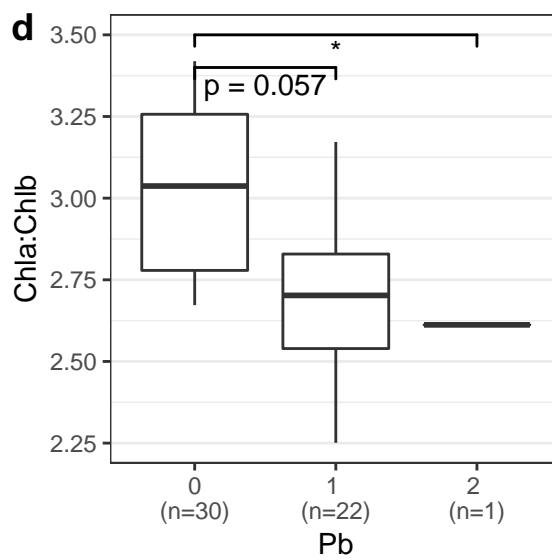
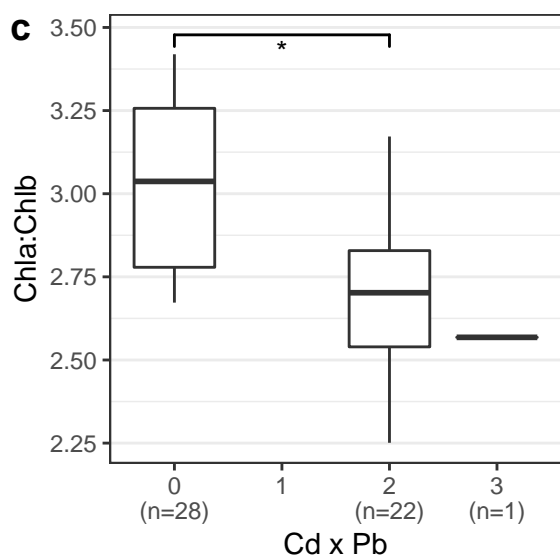
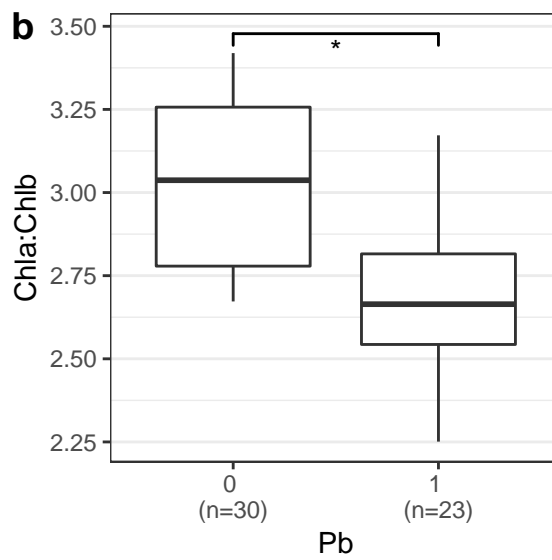
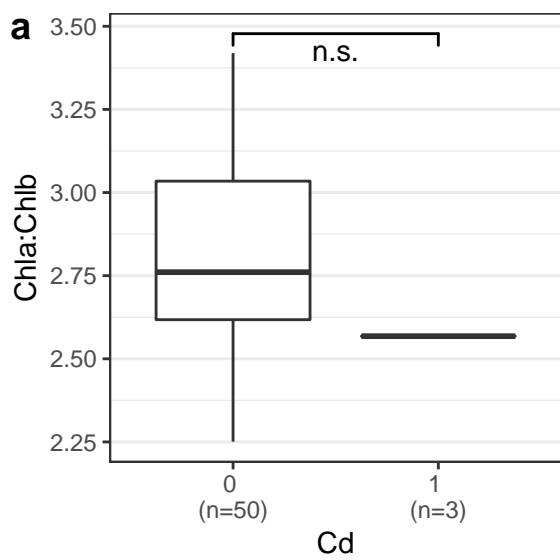
Trait	Mixed Model			Tukey's Test Class 0 – 1	
	Metal	F-value	P-value	Estimate	P-value
LMA	Cd	1.11	0.292	0.249	0.292
	Cr	6.68	0.010	-1.319	0.010
	Cu	0.16	0.691	0.284	0.691
	Ni	0.23	0.632	0.425	0.632
	Pb	67.08	<0.001	1.284	<0.001
	Zn	0.70	0.404	0.521	0.404
Fv/Fm	Cd	0.02	0.901	-0.0013	0.901
	Cr	0.01	0.905	0.0027	0.905
	Cu	0.01	0.911	0.0034	0.911
	Ni	0.08	0.772	-0.0109	0.772
	Pb	5.84	0.016	-0.0162	0.016
	Zn	0.08	0.784	-0.0074	0.784
Chl	Cd	2.31	0.138	18.091	0.138
	Pb	6.78	0.013	-9.238	0.013
Chla:Chlb	Cd	0.45	0.509	0.181	0.509
	Pb	23.58	<0.001	0.331	<0.001

Table 3. Mixed models for testing the effect of multi-level Cd×Pb and Pb contamination on leaf functional traits, including the leaf mass per area (LMA), Fv/Fm, total chlorophyll content (Chl) and Chla:Chlb ratio. The modeled random effects are city and site. Chlorophyll data were only available for a subset of the samples, where only Cd and Pb reached the threshold of contamination.

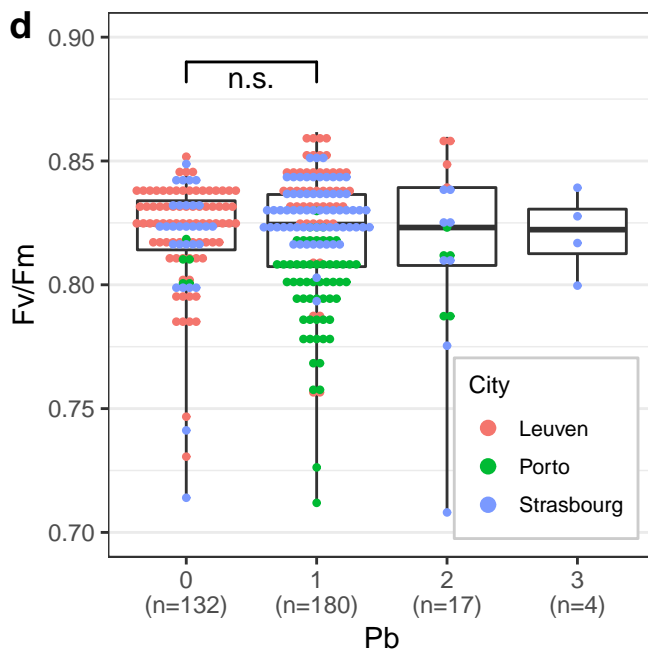
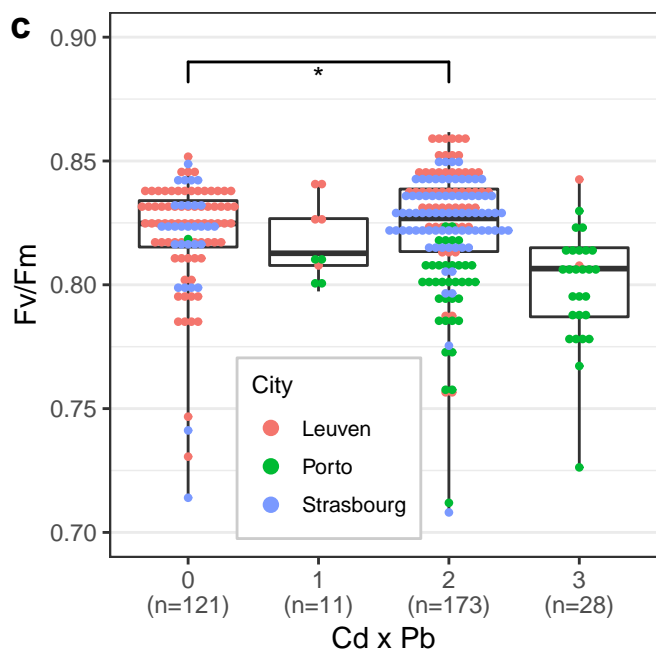
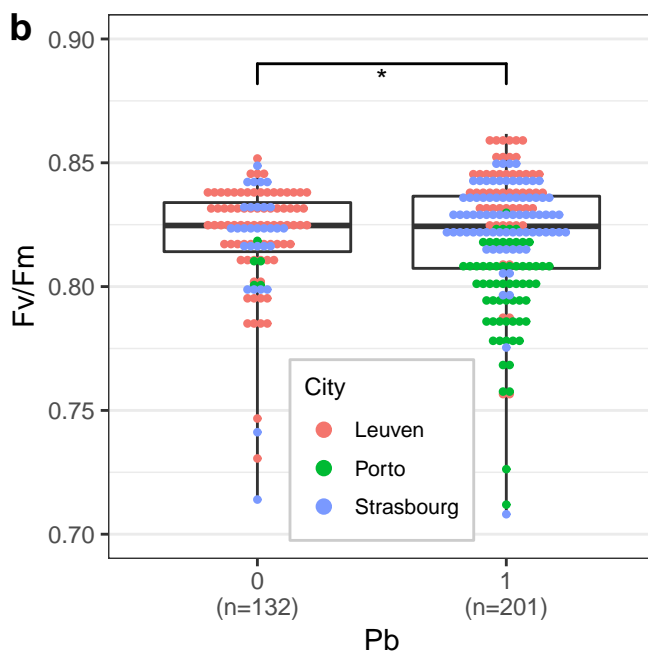
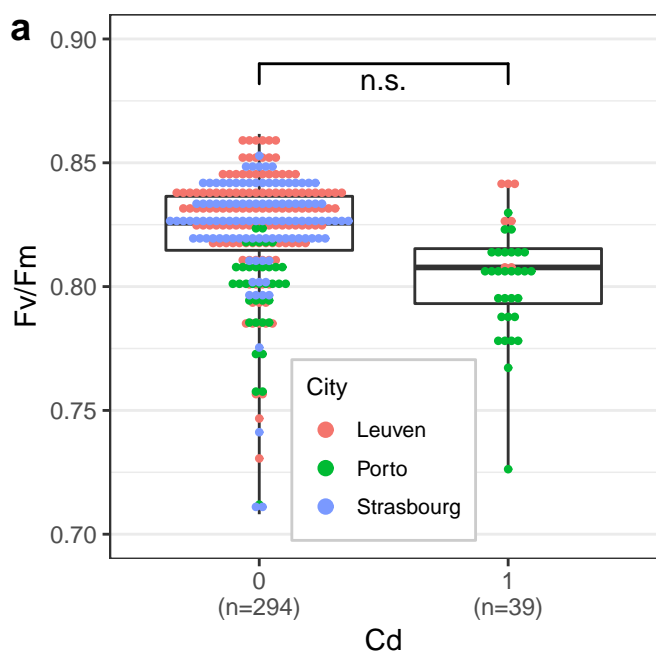
Trait	Mixed model		Tukey's Test												
	Metal	F-value	P-value	Class 0 – 1		Class 0 - 2		Class 0 - 3		Class 1 - 2		Class 1 - 3		Class 2 – 3	
				estimate	p	estimate	p	estimate	p	estimate	p	estimate	p	estimate	P
LMA	Cd×Pb	23.74	<0.001	0.025	1.000	1.256	<0.001	1.722	<0.001	1.231	0.006	1.698	0.001	0.466	0.246
	Pb	26.29	<0.001	1.21	<0.001	1.831	<0.001	2.444	<0.001	0.621	0.104	1.234	0.104	0.613	0.731
Fv/fm	Cd×Pb	2.42	0.066	-0.0211	0.661	-0.0184	0.044	-0.0143	0.713	0.0028	0.999	0.0069	0.987	0.0041	0.987
	Pb	2.00	0.113	-0.0168	0.070	-0.0109	0.863	-0.0106	0.980	0.0059	0.971	0.0062	0.996	0.0003	1.000
Chl	Cd×Pb	5.86	0.006			-10.275	0.014	12.558	0.495					22.834	0.108
	Pb	6.40	0.004	-8.108	0.057	-32.96	0.012			-24.852	0.070				
Chla:Chlb	Cd×Pb	11.47	<0.001			0.332	<0.001	0.319	0.319					-0.012	0.998
	Pb	12.01	<0.001	0.323	<0.001	0.495	0.072			0.172	0.709				

PRE-SCRIPT





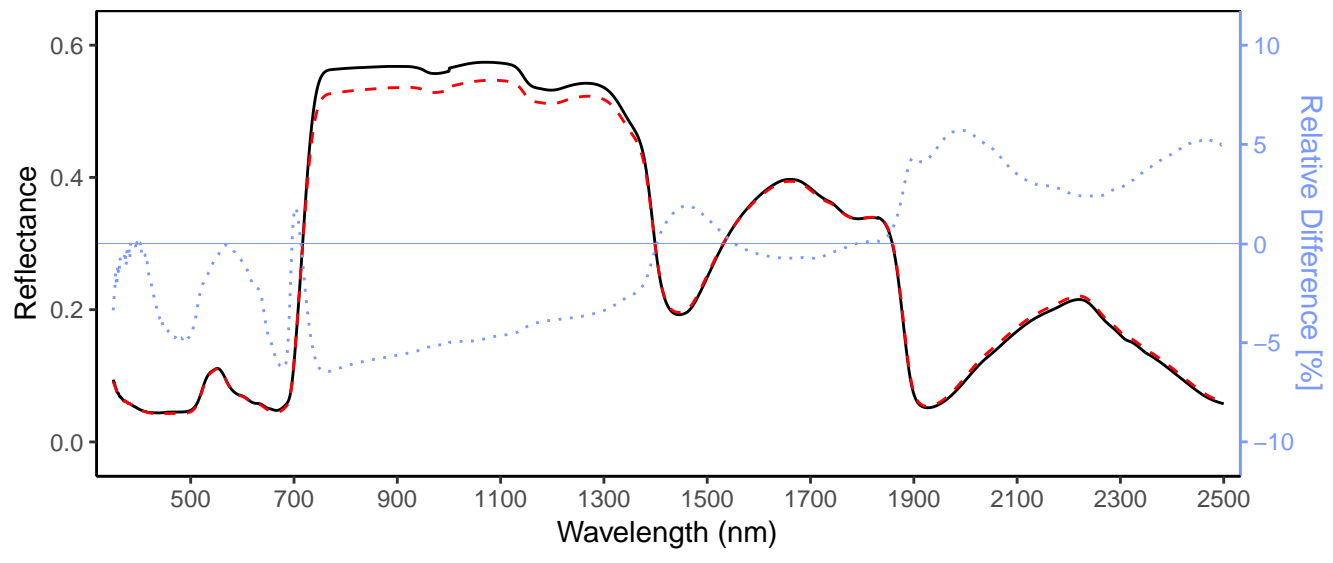
MANUSCRIPT



PRESCRIPT

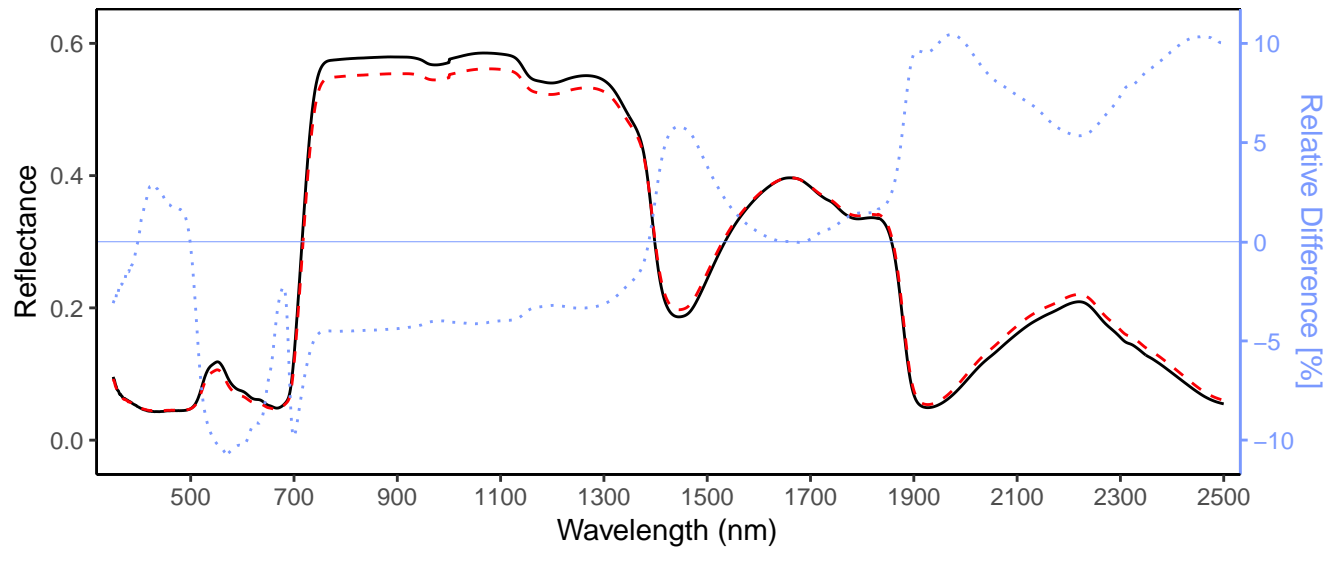
a

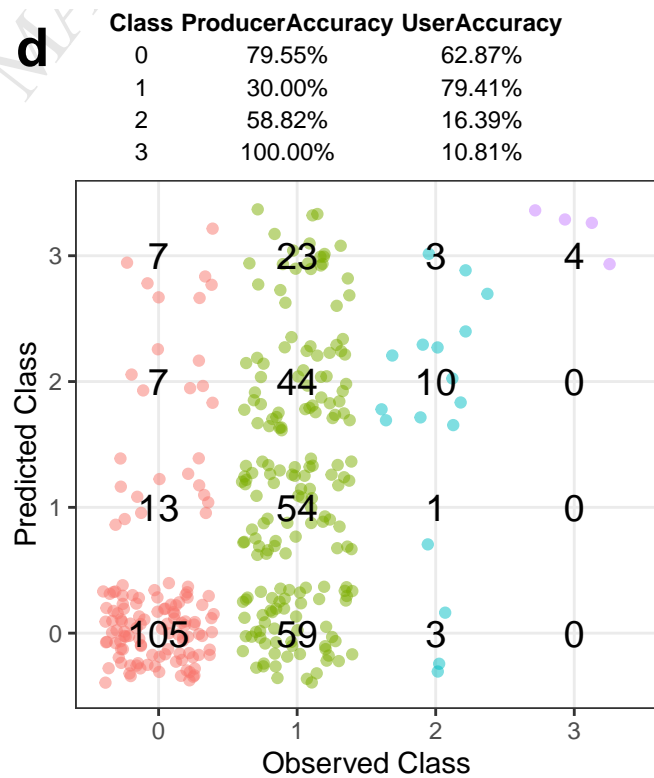
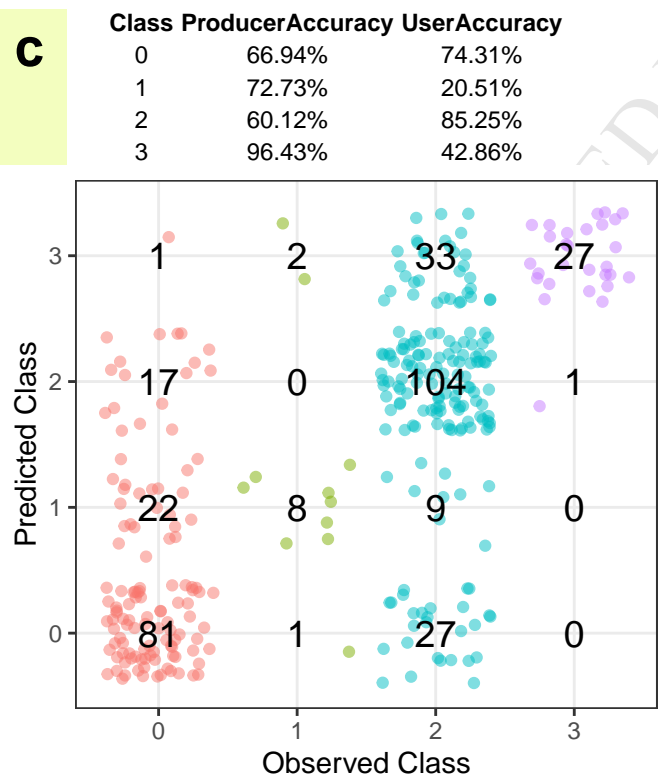
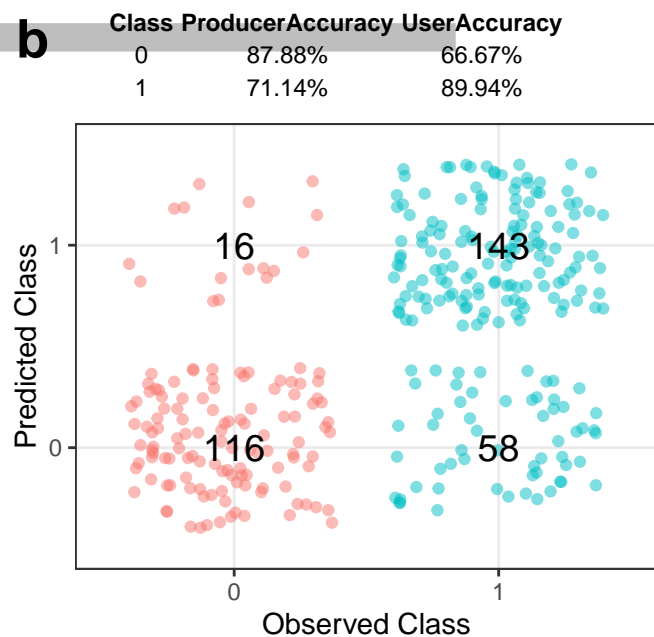
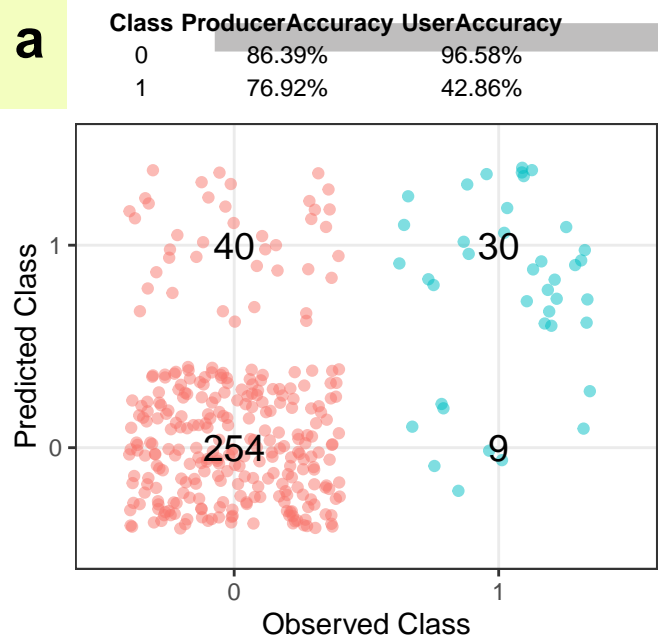
— Cd 0 - - - Cd 1 ····· Relative Difference

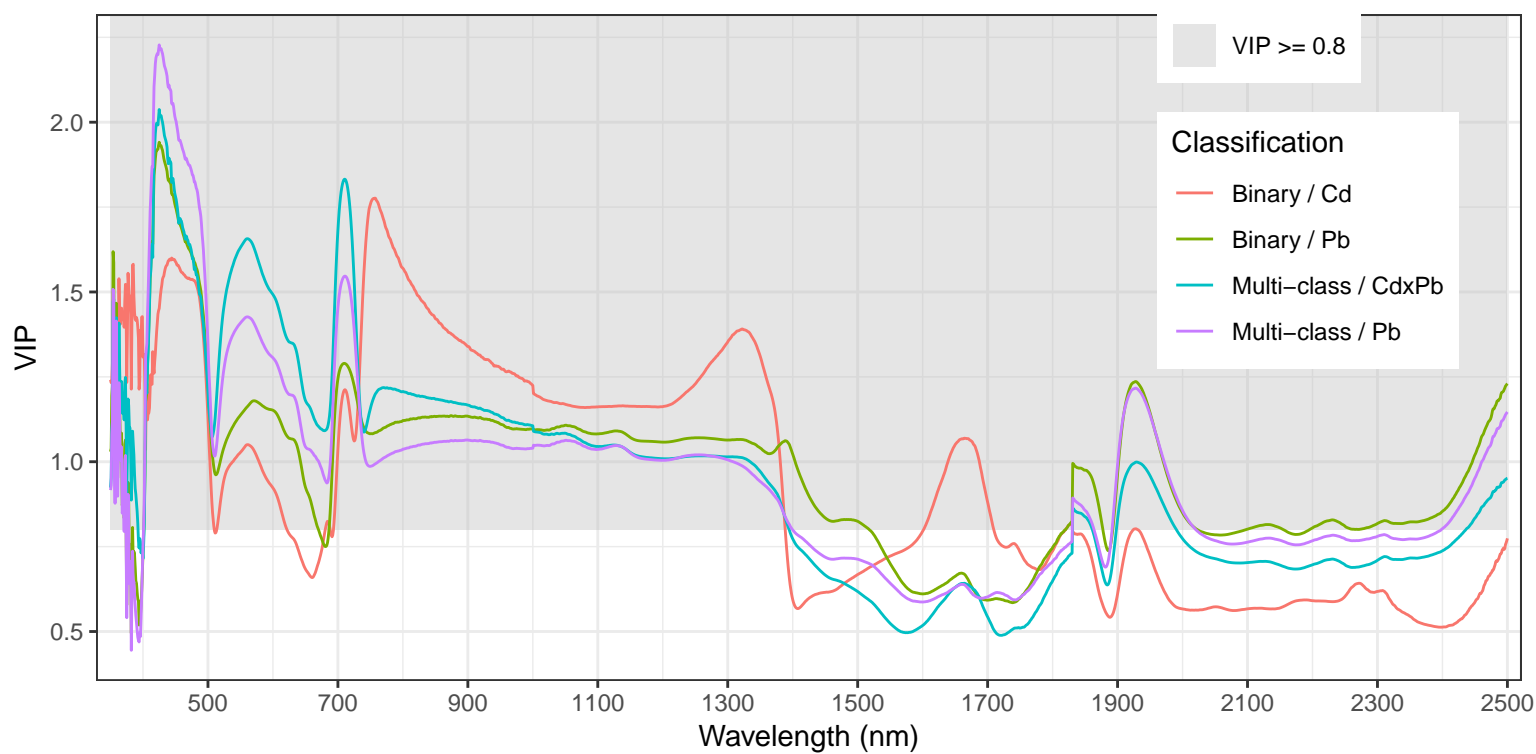


b

— Pb 0 - - - Pb 1 ····· Relative Difference







-
- Cd and Pb pollution in urban soils reduces the leaf mass per area of Tilia trees
 - Soil Cd and Pb pollution reduces the leaf chlorophyll a to b ratio of Tilia trees
 - Soil Cd and Pb pollution alters leaf spectral properties in the red-edge region
 - PLS-DA models based on leaf spectra allow for the detection of Cd and Pb pollution

ACCEPTED MANUSCRIPT

Comment citer ce document :

Yu, K., Van Geel, M., Ceulemans, T., Geerts, W., Ramos, M. M., Serafim, C., Sousa, N., Castro, P. M. L., Kastendeuch, P., Najjar, G., Ameglio, T., Ngao, J., Saudreau, M., Honnay, O., Somers, B. (2018). Vegetation reflectance spectroscopy for biomonitoring of heavy metal pollution in urban soils. *Environmental Pollution*, 243, 1912-1922. . DOI : 10.1016/i.envpol.2018.09.053